Solid Earth Discuss., 6, 2699–2733, 2014
www.solid-earth-discuss.net/6/2699/2014/
doi:10.5194/sed-6-2699-2014

Solid Earth Discussions
Open Access

High-precision relocation of seismic sequences above a dipping Moho: the case of the January–February 2014 seismic sequence in Cephalonia Isl. (Greece)

V. K. Karastathis, E. Mouzakiotis, A. Ganas, and G. A. Papadopoulos

National Observatory of Athens, Institute of Geodynamics, Lofos Nymfon, P.O. Box 20048, 11810, Athens, Greece

Received: 5 August 2014 – Accepted: 27 August 2014 – Published: 2 September 2014

Correspondence to: V. K. Karastathis (karastathis@noa.gr)

Published by Copernicus Publications on behalf of the European Geosciences Union.

Abstract

Detailed velocity structure and Moho mapping is of crucial importance for a high precision relocation of seismicity occurring out of, or marginally to, the geometry of seismological networks, such as at the boundary of converging plates. The crustal thinning from the plate boundary towards the back-arc area creates significant errors in accurately locating the earthquake, especially when distant seismic phases are included in the analysis. The case of the Cephalonia (Ionian Sea, Greece) sequence of January–February 2014 provided an excellent example where locations were greatly affected by the crustal thinning from the plate boundary at the Ionian sea towards the Aegean sea. This effect was examined in detail by testing various velocity models of the region in order to determine an optimal model. Our tests resulted in the adoption of a velocity model that resembles the crustal thinning of the region. Then, a relocation procedure was performed in the Cephalonia sequence for the time period from 26 January 2014 to 15 May 2014 by applying probabilistic non-linear location algorithms. The high-precision relocation resulted in an improved spatial distribution of the seismicity with respect to the preliminary locations and provided a reliable basis to examine seismotectonic implications of the Cephalonia sequence.

1 Introduction

On 26 January (13:55:42 and 18:45:08 GMT) and 3 February 2014 (3:08:44 GMT) western Cephalonia Isl., Ionian Sea (Greece), (Fig. 1) was ruptured by three strong earthquakes of magnitudes M_w6.0, M_w5.3 and M_w5.9, respectively (Table 1, Fig. 2). The two strongest earthquakes caused considerable damage in buildings and infrastructure as well as several types of ground failures (rock-falls, landslides, soil liquefaction) in Paliki peninsula, mainly in Lixouri town and the surrounding villages (Papadopoulos et al., 2014; Valkaniotis et al., 2014) (Fig. 1). The Peak Ground Acceleration (PGA) recorded in several localities at accelerometric stations, operated by the

SED
6, 2699–2733, 2014

National Observatory of Athens, Institute of Geodynamics (NOAGI) (NOA web report, 2014a, b) and the Institute of Engineering Seismology and Earthquake Engineering (EPPO-ITSAK web report 2014a, b) reached up to 0.56 and 0.77 g in Lixouri during the first and third earthquake, respectively. Since only three permanent seismic stations were existing in Cephalonia, on 28 and 29 January 2014, four portable seismic stations (Fig. 2) were installed by NOAGI in the aftershock zone of western Cephalonia with the aim to improve the monitoring capabilities.

Cephalonia was hit by many strong earthquakes in the past (Ambraseys, 2009, Papazachos and Papazachou, 2003). In the instrumental era of seismology the most important activity was a series of very strong, lethal earthquakes that ruptured eastern and central Cephalonia with the largest (M_s7.2) occurring on 12 August 1953. Large earthquakes occurred offshore west Cephalonia in 1972 and 1983 (Scordilis et al., 1985). The very high seismicity of Cephalonia is controlled by two major seismotectonic structures. The first is the right-lateral strike-slip Cephalonia Transform Fault Zone (CTFZ) comprising of the NNE-SSW trending Lefkada segment at north and the NE-SW trending Cephalonia segment at south (Louvari et al., 1999) (Fig. 1). The strong (M_w6.2) earthquake of 14 August 2003 ruptured offshore west Lefkada Isl. along the Lefkada segment of CTFZ (Fig. 1; Papadopoulos et al., 2003). Recently, Papadopoulos et al. (2014) based on the spatial pattern of the Cephalonia 2014 earthquake sequence proposed that the Lefkada segment does not terminate at the NW side of Cephalonia, as it was thought until now, but extents in the western Cephalonia (Fig. 1). A second major structure that controls the seismicity of the area is the north-easternward subduction of the Ionian segment of the Hellenic Arc beneath Cephalonia (Sachpazi et al., 2000), thus making up a highly complex seismotectonic setting.

The January–February 2014 seismic sequence is the first one that ruptured western Cephalonia and was instrumentally recorded by modern seismograph instruments. Therefore, the study of this sequence is of particular importance to better understand the seismicity of Cephalonia. To this aim we performed a high-precision relocation of the seismic sequence of more than 3300 events of magnitude range M1.0–6.0, extend-

SED
6, 2699–2733, 2014

ing from 26 January 2014 up to 15 May 2014. Then, relocation results were utilized to interpret the seismotectonics of the 2014 activity as well as the geometry and kinematics of the CTFZ major structure.

2 The problem of location

The routine determination of earthquake hypocentral parameters usually suffer from significant errors.

More specifically, the main sources of errors for an accurate determination of the hypocentral parameters are: (a) the false identification of the seismic phases, (b) the insufficient number of phases, (c) the deficient azimuthal coverage of the seismographic network and finally (d) the use of non-effective seismic velocity models that are usually oversimplified (often one-dimensional) without adequate information for the velocity structure and the lateral velocity heterogeneities. It is a common practice that unified, regional 1-D velocity models are in use, which is also the case of NOAGI for the daily seismicity monitoring of Greece (see Fig. 3). Such velocity models deviate considerably from the local velocity structure of an area, especially at the geometrical edge of the area which is covered by the network.

Although it is feasible to derive reliable seismic velocity models for areas in a local scale, through the implementation of nonlinear inversion techniques that simultaneously invert microseismicity travel-time data for the hypocentral parameters and seismic velocity determination (Kissling et al., 1994; Kissling, 1995; Thurber, 1993; Koulakov, 2009), it is difficult to perform this practice in a regional scale. Additionally, information coming from crustal seismic surveys is usually useful to build only local velocity models. The crustal mapping based on gravity models suffers from intrinsic ambiguity and the resolution of the seismic velocity global models is too low (Koulakov and Sobolev, 2006).

Inaccurate hypocenter determinations become more acute in the presence of strong structural anomalies and variations which make a structure much different from a hori-

SED
6, 2699–2733, 2014

zontally layered Earth. For example, the crustal thickness is strongly affected in areas situated in the vicinity of convergent plate boundaries. This is the case of the thick continental Aegean crust in the vicinity of the Hellenic subduction zone. In fact, the compressional regime along the Hellenic Arc leads to folding and thin-skinned tectonics as well as to the creation of the Mediterranean ridge, which evolved to an accretionary prism, and to subsequent thickening of the crust (Underhill, 1989; Yem et al., 2011). Crustal surveys have shown that in western Greece, where the oceanic crust of the African plate is sliding beneath the Aegean area, the continental crustal thickness exceeds 40 km and becomes progressively thinner to the east (Makris, 1978; Tsokas and Hansen, 1997; Papazachos and Nolet, 1997; Tiberi et al., 2001; Karagianni et al., 2005; Pearce et al., 2012). At the South Aegean Sea region the crustal thickness reaches values as low as 20 km or less (Makris 1975, 1976, 1977; Bohnhoff et al. 2001; Tirel et al., 2004). Thus, when an earthquake occurs in the thick part of the crust and the wave-paths of the first arriving waves pass through the Moho that progressively becomes shallower, the travel-time errors may increase considerably with the increase of the epicentral distance. In contrast, shallower events are not so strongly affected, particularly in short epicentral distances since only *Pg* phases are actually picked. This structure causes an asymmetrical shape to the head-wave wavefront. Due to this structure, the adoption of a 1-D velocity model (see NOA-IG model in Fig. 3) can cause systematic travel time residuals in the events location.

3 Analysis of seismological data

The Cephalonia 2014 seismic sequence was examined exactly in this context. The first strong earthquake of 26 January 2014 was recorded by the permanent stations of the HUSN (Hellenic Unified Seismological Network; http://www.gein.noa.gr/en/networks/husn/) before the installation of the portable network in Cephalonia. The focus of that event was preliminary determined by NOAGI at a location situated about 5 km NNE from the city of Argostoli and at focal depth of h = 21 km (Fig. 2) (Table 1). This location

SED
6, 2699–2733, 2014

falls clearly outside of the aftershock cloud as well as far from the Lixouri town, where the macroseismic epicenter was placed according to the field observations performed by Papadopoulos et al. (2014) (Fig. 2). The epicentral area is situated at the geometrical edge of the permanent network in the sense that no stations were situated to the west of the earthquake focus. Consequently, the azimuthal coverage was poor, leading to unstable location solutions. In addition, the preliminary solution included several phases from significantly large epicentral distances extending up to 360 km, where the crustal thickness was significantly smaller than that in the subduction regime of western Cephalonia. The 1-D model used by NOAGI (Fig. 3), with the Moho boundary placed at 40 km, could not match *Pn* phase data from areas of thin crust, particularly at large epicentral distances. Therefore, significant errors were involved and consequently the epicenter of the first strong earthquake was shifted substantially to the east. Its aftershocks, however, were not shifted significantly because of their small magnitudes that limited epicentral distances over which they were recorded. In a next paragraph it is explained more precisely how errors are introduced in the epicentral solution.

Regarding the preliminary epicenter of the strong (M_w5.3) aftershock of 26.1.2014 (18:45:08 GMT), it is noticeable that it was located in a better agreement with the macroseismic epicenter (Fig. 2) although it was calculated before the installation of the portable network in Cephalonia. This is explained by the fact that its actual focal depth was shallower than that of the first strong earthquake. It is also worth mentioning that two seconds after the first strong shock of the 26 January 2014, another strong aftershock occurred. Unfortunately, the waveform of this event partially overlapped with the waveform of the first strong shock, making an accurate estimation of its local and moment magnitudes quite difficult. A rough estimation of its duration magnitude gives M_d5.0. This is consistent with the accounts of local people reporting that a few seconds after the first major event another shock was strongly felt in Cephalonia.

After the installation of the portable network in western Cephalonia the maximum azimuthal gap was decreased significantly, becoming less than 180° for most of the seismic events. The preliminary focus of the strong earthquake (M_w5.9) of 3 Febru-

SED
6, 2699–2733, 2014

ary 2014 was located at shallower depth (h = 11 km, Table 1) but within the aftershock cloud (Fig. 2) and at a position close to its macroseismic epicenter which again was placed (Papadopoulos et al., 2014) in Lixouri town.

To effectively relocate the hypocenter data of the sequence one may use a velocity model resembling as much as possible the real velocity structure. An effective model can compensate for most of the systematic time residuals created at distant stations. An alternative method is to use a 1-D model, having found however the epicentral distance range where the effect of the inclined Moho does not considerably affect the location accuracy. This approach limits the seismic phases taken into account. It is reasonably expected that the two different approaches should lead to quite similar results.

4 Selection of velocity model – relocation of the Cephalonia 2014 earthquake sequence

For western Greece, including the area of Cephalonia, only few seismic velocity models have been proposed (Hirn et al., 1996; Haslinger et al., 1999; Sachpazi et al., 2000). The model proposed by Hirn et al. (1996) was directly based on the results of the crustal seismic surveys carried-out during 1992 in the frame of the project STREAMERS. The profile ION-7, with bearing of N62° E, was conducted offshore between Cephalonia and Zakynthos (Zante) islands having total length of 180 km, starting from the deep Ionian basin and reaching the western Gulf of Patras (see maps in Hirn et al., 1996). For the data acquisition the Geco-Prakla's M/V *Bin Hai 511* was used with a 36-airgun tuned array (for processing details see also in Kokinou et al., 2005). The 30-fold seismic profile acquired, provided useful information for the shallower structure. However, no precise information was gathered for the Moho interface. To get a rough estimate of the Moho depth, Hirn et al. (1996) performed ray-tracing modeling of the wide-angle traveltime data, recorded at distant on-shore stations positioned at the Greek mainland. Those stations were located only at the eastern side of the profile. Furthermore assumptions were made for the velocity values beneath the 7 km depth.

SED
6, 2699–2733, 2014

Thus, these authors discussed a model with the lower crustal interface (V_p between 5.8 and 6.8 km s^{-1}) at 15 km depth and the Moho boundary at 25 km. Since the structure in this model was almost horizontal, the 1-D model of Fig. 3 can be easily derived.

The velocity model of Haslinger et al. (1999) (Fig. 3) was built for the region at the east of Lefkada Isl., western Greece, which as regards to the Cephalonia 2014 sequence, concentrates a high percentage of the ray-paths between the earthquakes and the stations. This model was built as a "1-D minimum velocity model" for this region by VELEST algorithm (Kissling et al., 1994; Kissling, 1995) and used in a following stage as initial model in the local earthquake tomography method and SIMULPS code (Thurber, 1993; Eberhart-Phillips, 1990, 1993), implemented to calculate the 3-D crustal velocity structure. The SIMULPS code uses a linearized damped least-square inversion to solve the non-linear problem of the hypocentral location and velocity model. Because of this non-linear nature of the problem, the initial velocity model and the initial hypocenter locations in the inversion procedure should be as close as possible to their true values. The "1-D minimum velocity model" calculated by the VELEST algorithm can provide a good approximation and be used as an initial velocity model. The minimum 1-D velocity models are usually used for seismicity relocation (e.g. Lippitsch et al., 2005; Ganas et al., 2014).

The model proposed by Sachpazi et al. (2000) (Fig. 3) was also created by the VELEST algorithm in order to be used as initial model in a 3-D local earthquake tomography performed to determine the velocity structure of the area under study. The procedure for the construction of a 1-D minimum velocity model is highly dependent on the selection of an initial model (Karastathis et al., 2011) and, therefore, it is usually based on the results of seismic profiles. Sachpazi et al. (2000) based their initial model on the seismic profiles presented by Hirn et al. (1996).

For the adoption of an appropriate seismic velocity model we compared the three 1-D models mentioned above (Fig. 3). As we will see later in detail, the model that performed better was the one proposed by Haslinger et al. (1999). With a vertical velocity gradient based on Haslinger et al. (1999) we finally constructed, tested and adopted

SED
6, 2699–2733, 2014

a 2-D velocity model with a non-horizontal Moho boundary based on Papazachos and Nolet (1997). Fig. 4 shows the vertical cross-section of the 2-D model.

Before comparing the performance of these models, we examine the influence on the location procedure of the non-horizontal Moho boundary in the Aegean region. More specifically, in order to assess the impact of the errors imposed in the earthquake location procedure by the adoption of a simplified 1-D model, in the presence of a non-horizontal Moho structure, we constructed synthetic arrival times for the adopted model using the 3-D version of the eikonal finite-difference scheme of Podvin and Lecomte (1991) and estimated the time differences for both a horizontal and a non-horizontal Moho structure. The velocity gradient was based on Haslinger et al. (1999). The 2-D model with the non-horizontal Moho boundary is shown in Fig. 4 and the results of the comparison with the respective 1-D are depicted in Fig. 5. As one may expect, the time difference is zero only when the first arrivals are due to the *Pg* seismic phases. Obviously, the shallower events, with focal depth between 5 and 10 km are not affected or affected only slightly, particularly when they do not bare enough energy to travel at long epicentral distances. As a result, the majority of the shallow aftershocks remain unaffected. In contrast, the influence is higher for the deeper and stronger events, such as the first strong earthquake of 26 January 2014. For this strong earthquake three different epicenters were calculated with the use of the 1-D model (with the inclusion or the exclusion of distant phases) and with the 2-D model (with all phases) (Fig. 6). It can be seen how the simplified 1-D velocity model affects the epicenter location when distant phases are taken into account. The error decreases when distant phases are omitted.

We concluded that for lack of reliable knowledge regarding the structure and velocity of the Moho boundary and in the presence of poor azimuthal seismographic coverage, it is preferable to limit the range of the epicentral distances of stations used and to base the location mostly on the *Pg* phases.

The data processing has been performed by the NonLinLoc algorithm (Lomax et al., 2000) that follows a non-linear earthquake location method giving a complete prob-

SED
6, 2699–2733, 2014

abilistic solution expressed in terms of a posterior density function (PDF) (Tarantola and Valette, 1982). The function is calculated using the Equal Differential Time (EDT) likelihood function and depicted by confidence ellipsoids. Therefore, the highest the confidence of the velocity model, the smaller the ellipsoids of the event locations. This probabilistic approach is characterized by strong advantages as compared with linearized methods. More precisely, the EDT function provides a more reliable uncertainty estimate, especially in the presence of outliers, than the conventional least-squares L1 and L2 norms for the misfit calculation between the observed and calculated travel times. Another advantage of the method is that it is independent on the origin time, so the 4-D problem of hypocenter location reduces to a 3-D search over spatial location of the hypocenter (latitude, longitude, depth). The NonLinLoc algorithm can also use 2-D and 3-D velocity models.

For the relocation of the Cephalonia 2014 aftershock sequence we used NOAGI phase dataset consisting of more than 44 000 *P* wave and 24 000 *S* wave arrivals for the time interval from 26 January 2014 to 15 May 2014 inclusive. Phase data from distant stations ($\Delta > 120$ km) were excluded. It should be noted, however, that small magnitude events remained unaffected since they could hardly be identified at greater epicentral distances anyway.

We compared both the 2-D and 1-D versions of the adopted model with the three models proposed by previous authors (Fig. 3). For the comparison we selected events with at least six *P* and one *S* wave arrivals and azimuthal gap lower than 180°. The station delays were calculated and applied to the location procedure. Station corrections compensate for the effect of the station local geology, which could not be taken into account by the use of 1-D velocity model. The adopted model succeeds in producing a more compact horizontal projection (Fig. 7) and verifies that the aftershock sequence, trending NNE–SSW, covers only the western part of Cephalonia at a length of about 35 km and maximum lateral width of about 10 km. It is noteworthy that the relocated aftershock area nearly coincides with the main part of the macroseismic field that is the area covered by the isoseismal of level V, which is also the area of ground failures pro-

SED
6, 2699–2733, 2014

duced by the strong earthquakes of 26 January and 3 February 2014. (Papadopoulos et al., 2014).

The model of Haslinger et al. (1999) performs significantly better than those of Hirn et al. (1996), Sachpazi et al. (2000) as well as that of NOAGI as it comes out from histograms of horizontal and vertical location errors (Table 2 and Figs. 8 and 9). The vast majority (about 80 %) of the events relocated with the adopted model have horizontal error less than 900 m. Moreover, the 52 % of the relocated events have a horizontal error less than 600 m (Table 2). As we can also see in the same table the original 1-D model of Haslinger et al. (1999) is not notably inferior in contrast with the other three models which produced significantly larger errors. Similar results can be seen also in Fig. 9 that depicts the vertical error distribution (see also Table 2).

For the first 15 km of depth the model of Haslinger et al. (1999) has similar velocity values with the model proposed by Hirn et al. (1996) which was produced from reliable data of seismic reflection profiles. However, there is an obvious discrepancy at depths greater than 15 km. This might be explained by the fact that for these depths, Hirn et al. (1996) used results only from ray-tracing modeling based on common receiver data only from one side (eastern part) of the seismic traverse. In contrast, Haslinger et al. (1999) did not considered an abrupt increase in the velocity structure at 15 km depth and proposed a Moho boundary at 40 km, whereas Hirn et al. (1996) used a Moho depth at 25 km. Very likely the shallow Moho boundary is the main reason of the poor relocation results we obtained from the model of Hirn et al. (1996).

The aftershock focal depths calculated by various models also show significant variations (Fig. 10). The adopted model, as well as that of Haslinger et al. (1999), have the vast majority of focal depths between 6–14 km. The model of Sachpazi et al. (2000) calculated a significant percentage of the hypocenters at depths between 4–6 km and a very low percentage with depths greater than 12 km. No hypocenters with unrealistic depth values (< 4) were calculated by the models based on Haslinger et al. (1999).

SED
6, 2699–2733, 2014

5 Seismotectonic implications and discussion

The spatial distribution of the relocated earthquake sequence (Fig. 7a) confirms that the 2014 earthquake activity covers only the western part of Cephalonia Island trending from NNE to SSW at a length of about 35 km and maximum lateral width of c. 10 km. No earthquake activity was developed offshore western Cephalonia. As a consequence, the January–February 2014 earthquake sequence can hardly be seismotectonically associated with the Cephalonia segment of the major right-lateral strike-slip structure of the Cephalonia Transform Fault Zone (CTFZ), as the latter was proposed by Louvari et al. (1999). On the contrary, the aftershock pattern implies that the 2014 activity ruptured western Cephalonia due to on-shore strike-slip faulting. One possible scenario is that the activated strike-slip faults comprise the southern prolongation of the NNE-SSW trending Lefkada segment of the CTFZ. Papadopoulos et al. (2014) suggested that the Lefkada CTFZ segment does not terminate offshore NW Cephalonia, as proposed by previous authors (Louvari et al., 1999), but extents further in western Cephalonia. Another scenario is that the activated strike-slip faults comprise segments of a 30 km nearly N–S trending fault zone that splits the island in two parts: the western and eastern ones. The consequence is that western Cephalonia appears as a seismotectonic block independent from the eastern Cephalonia that hosted the sources of the large 1953 earthquakes.

The space-time evolution of the 2014 sequence (Fig. 11), based on the high-precision relocated earthquake catalogue that we produced, indicates that soon after the occurrence of the first strong earthquake of 26 January 2014 the aftershock area was already well-shaped. No further expansion of the aftershock area was observed, neither after the 29th of January, when the portable network was installed, nor after the occurrence of the strong earthquake of 3 February 2014.

The Cephalonia 2014 sequence is geographically distributed in two clusters (Figs. 7a, 12). The first is small being of a length of the order of 10 km and occupying the north side of the aftershock cloud. The other extends in the central and south

SED
6, 2699–2733, 2014

sides, thus leaving an apparent spatial gap between the two clusters. Papadopoulos et al. (2014) suggested that the area of the 2014 gap had already ruptured by the strong (M_w5.5) strike-slip earthquake of 25 March 2007. However, no temporal relation was found between these two clusters and the occurrence of the strong events of 26 January and 3 February 2014. The north cluster abuts but does not overlap with the southern side of the aftershock area of the 2003 Lefkada Isl. strong (M_w6.2) mainshock (Papadopoulos et al., 2003) (see also Fig. 13). Besides, the foreshock activity that preceded the first strong earthquake of 26 January 2014 by about four days was recorded exactly in the area of the north (small) aftershock cluster (Papadopoulos et al., 2014). This may indicate that the 2014 activity was initiated at the northern part of the aftershock area where the 2003 Lefkada Isl. activity diminished. Therefore, we observe that a shallow tectonic structure exists in the area of Myrtos Gulf, possibly a near-vertical fault striking WNW-ESE that is perpendicularly to the NNE-SSW strike of the Lefkada 2003 and the Cephalonia 2014 aftershock areas. This fault, which probably controlled the initiation of the 2014 sequence, can be seen in the NNE-SSW cross-section in Fig. 14c that depicts clearly the vertical geometry of the EW cross-fault at Myrtos Gulf, at depths 5–12 km. Evidence also comes from the space-time evolution of the relocated 2014 sequence (Fig. 11) but further examination is needed.

With the relocation applied, the foci of the three strongest earthquakes of the sequence shifted at shallower depths, while the first strong earthquake of 26 January 2014 shifted also towards WNW with respect to the preliminary determinations (Table 1). The thickness of the seismogenic layer does not exceed 16 km. That the 2014 aftershock area was well-formed from the very beginning without spatial expansion after the strong earthquake of 3 February 2014 provides evidence that this earthquake ruptured within the aftershock volume of the 26 January 2014 earthquake which was the largest event of the sequence. From this point of view we may consider that the 3 February event was the strongest aftershock of the sequence that ruptured at shallower depth and at different fault from that of the mainshock of 26 January 2014.

SED
6, 2699–2733, 2014

To further control the fault patterns associated with the 26 January and 3 February earthquakes we constructed two respective vertical cross sections as shown in Fig. 14. One may observe that in the section corresponding to the mainshock of 26 January, the aftershocks up to 30 January included in a ±4 km wide zone seem rather arranged in a plane of nearly N–S direction and dip of about 65° to the east (Fig. 14a). The preferred fault-plane adopted by Papadopoulos et al. (2014) and Valkaniotis et al. (2014) is of strike 23° and dip 68° to the east, which is consistent with the geometry represented by the vertical section. However, the vertical section through the hypocentre of the 3 February 2014 event (Fig. 14b) shows that the fault plane strikes nearly N–S but its dip is about 65° to the west. The geometry of this fault plane is compatible with the fault plane that dips 56° to the west according to the focal mechanism computed by the GFZ (183° / 56° / 138°; reported at the European – Mediterranean Seismological Centre (EMSC) website http://www.emsc-csem.org/Earthquake/mtfull.php?id=357329). The western dip in combination with the oblique-slip rake may result in uplift of the hanging-wall (western) part of the N–S fault during co-seismic motion.

Our relocation procedure suggests a different fault model than that of Karakostas et al. (2014; their Fig. 8) who suggested a right-step of CTFZ, onshore Paliki peninsula. On the contrary, we image the activation of two, blind strike-slip faults along the N-S axis at Myrtos Gulf – Lixouri line, possibly overlapping with a left step. The 26 Janaury 2014 activated fault (Fig. 14a) is in agreement with the blind fault model of Valkaniotis et al. (2014). Such a fault configuration may explain the co-seismic uplift seen on Paliki Peninsula in InSAR data (Boncori et al., manuscript submitted to SRL) as our relocation data in the epicentral region of the 3 February 2014 event point to a west-dipping fault (Fig. 14b). If this is the case, then the hanging wall of this fault moved upwards during co-seismic motion as it is known that Cephalonia region is in state of compression with max. horizontal stress oriented at N78E (+/ – 9 degrees; Ganas et al., 2013), as determined from GPS data. In addition, Lagios et al. (2012) obtained a N-S discontinuity in their horizontal velocity field (see Fig. 4c of Lagios et al., 2012) across the Gulf

SED
6, 2699–2733, 2014

of Argostoli, which may be indicative of a crustal block boundary or a large fault zone beneath the Gulf.

Acknowledgements. Thanks are extended to the Acting Director and the staff of the Institute of Geodynamics for the daily processing of many seismic phases as well as for the installation of the portable network in Cephalonia. Thanks are also due to the topical editor of the journal, Takaaki Taira, for his suggestions on improving the original manuscript.

References

Ambraseys, N.: Earthquakes in the Mediterranean and Middle East. Cambridge University Press, New York, 8, 4333–4355, 2009.

Bohnhoff, M., Makris, J., Papanikolaou, D., and Stavrakakis, G.: Crustal investigation of the Hellenic subduction zone using wide aperture seismic data, Tectonophysics, 343, 239–262, 2001.

Eberhart-Phillips, D.: Three-dimensional P and S velocity structure in the Coalinga Region, California, J. Geophys. Res., 95, 15343–15363, 1990.

Eberhart-Phillips, D.: Local earthquake tomography: earthquake source regions, in: Seismic Tomography: Theory and Practice, edited by: Iyer, H.M., and Hiahara, K., Chapman and Hall, London, 613–643, 1993.

EPPO-ITSAK: The 26 January 2014 Earthquake in Cephalonia, Preliminary Report, by EPPO-ITSAK (in Greek), (http://www.slideshare.net/itsak-eppo/2014-0127-kefaloniaeqpreliminaryreporta), 2014a.

EPPO-ITSAK:. Strong Ground Motion of the February 3, 2014 Cephalonia Earthquake: Effect on Soil and Built Environment in Combination with the 26 January , 2014 Event. (http://www.slideshare.net/itsak-eppo/20140203-kefaloniaeq-report-en), 2014b.

Ganas, A., Karastathis, V., Moshou, A., Valkaniotis, S., Mouzakiotis, E., and Papathanassiou, G.: Aftershock properties and seismotectonic setting of the 7 August 2013 moderate earthquake in Kallidromon Mountain, central Greece, Tectonophysics, 617, 101–113, 2014.

Ganas, A., Marinou, A., Anastasiou, D., Paradissis, D., Papazissi, K., Tzavaras, P., and Drakatos, G.: GPS-derived estimates of crustal deformation in the central and north Ionian Sea, Greece: 3-yr results from NOANET continuous network data, J. Geodynamics, 67, 62–71, 2013.

SED

6, 2699–2733, 2014

Haslinger, F., Kissling, E., Ansorge, J., Hatzfeld, D., Papadimitriou, E., Karakostas, V., Makropoulos, K., Kahle, H. G., and Peter, Y.: 3-D crustal structure from local earthquake tomography around the Gulf of Arta (Ionian region, NW Greece), Tectonophysics, 304, 201–218, 1999.

Hirn, A., Sachpazi, M., Siliqi, R., Bride, J. M., Marnelis, F., and Cernobori, L., and STREAMERS-PROFILES group: A traverse of the Ionian islands front with coincident normal incidence and wide-angle seismics, Tectonophysics, 264, 35–49, 1996.

Karagianni, E. E., Papazachos, C. B., Panagiotopoulos, D. G., Suhadolc, P., Vuan, A., and Panza, G. F.: Shear velocity structure in the Aegean area obtained by inversion of Rayleigh waves, Geophys. J. Int., 160, 127–143, 2005.

Karakostas, V., Papadimitriou, E., Mesimeri, M., Gkarlaouni, C., and Paradisopoulou, P.. The 2014 Kefalonia doublet (M_w6.1 and M_w6.0), Central Ionian Islands, Greece: Seismotectonic implications along the Kefalonia transform fault zone, Acta Geophysica, 1–16, 2014.

Karastathis, V. K., Papoulia, J., Di Fiore, B., Makris, J., Tsambas, A., Stampolidis, A., and Papadopoulos, G. A.: Deep structure investigations of the geothermal field of the North Euboean Gulf, Greece, using 3-D local earthquake tomography and Curie point depth analysis, J. Volcanol. Geotherm. Res., 206, 106–120, 2011.

Kissling, E.: Velest User's Guide, Internal report, Institute of Geophysics, ETH, Zurich, 1995.

Kissling, E., Ellsworth, W. L., Eberhart-Phillips, D., and Kradolfer, U.: Initial reference models in local earthquake tomography, J. Geophys. Res., 99, 19635–19646, 1994.

Kokinou, E., Kamberis, E., Vafidis, A., Monopolis, D., Ananiadis, G., and Zelelidis, A.: Deep seismic reflection data Greece: a new crustal model for the Ionian sea, J. Pet. Geol., 28, 81–98, 2005.

Koulakov, I.: LOTOS code for local earthquake tomographic inversion: benchmarks for testing tomographic algorithms, B. Seism. Soc. Am., 99, 194–214, 2009.

Koulakov, I. and Sobolev, S. V.: Moho depth and three-dimensional *P* and *S* structure of the crust and uppermost mantle in the Eastern Mediterranean and Middle East derived from tomographic inversion of local ISC data, Geophys. J. Int., 164, 218–235, 2006.

Lagios, E., Papadimitriou, P., Novali, F., Sakkas, V., Fumagalli, A., Vlachou, K., and Del Conte S.: Combined Seismicity Pattern Analysis, DGPS and PSInSAR studies in the broader area of Cephalonia (Greece), Tectonophysics, 524, 43–58, 2012.

SED
6, 2699–2733, 2014

Lippitsch, R., White, R. S., and Soosalu, H.: Precise hypocentre relocation of microearthquakes in a high temperature geothermal field: the Torfajökull central volcano, Iceland, Geophys. J. Int, 160, 371–388, 2005.
Lomax, A., Virieux, J., Volant, P., and Berge-Thierry, C.: Probabilistic earthquake location in 3-D and layered models, in: Advances in Seismic Event Location, edited by: Thurber, C. H. and Rabinowitz, N., Kluwer Academic Publishers, Dordrecht/Boston/London, 101–134, 2000.
Louvari, E., Kiratzi, A. A., and Papazachos, B. C.: The CTF and its extension to western Lefkada Island, Tectonophysics, 308, 223–236, 1999.
Makris, J.: Crustal Structure of the Aegean Sea and the Hellenides Obtained from Geophysical Survey, J. Geophys., 41, 441–443, 1975.
Makris, J.: A dynamic model of the Hellenic arc deduced from geophysical data, Tectonophysics, 36, 339–346, 1976.
Makris, J.: Geophysical Investigations of the Hellenides, Hamburger Geophysikalische Einzelschriften, edietd by: Söhne, G. M. L. W., 1977.
Makris, J.: The crust and upper mantle of the Aegean region from deep seismic soundings, Tectonophysics, 46, 269–284, 1978.
NOA web report: http://www.gein.noa.gr/Documents/pdf/Cefalonia_20140126_preliminary_web.pdf (last accessed: 4 June 2014), 2014a.
NOA web report: http://www.gein.noa.gr/Documents/pdf/Cefalonia_20140203_preliminary_web.pdf (last accessed: 4 June 2014), 2014b.
Papadopoulos, G. A., Karastathis, V. K., Ganas, A., Pavlides, S., Fokaefs, A., and Orfanogiannaki, K.: The Lefkada, Ionian Sea (Greece), shock (M_w6.2) of 14 August 2003: Evidence for the characteristic earthquake from seismicity and ground failures, Earth Planet. Space, 55, 713–718, 2003.
Papadopoulos, G. A., Karastathis, V. K., Koukouvelas, I., Sachpazi, M., Baskoutas, I., Chouliaras, G., Agalos, A., Daskalaki, E., Minadakis, G., Moschou,A., Mouzakiotis, E., Orfanogiannaki, A., Papageorgiou, A., Spanos D., and Triantafyllou, I.: The Cephalonia, Ionian Sea (Greece), sequence of strong earthquakes of January–February 2014: a first report, Res. Geophys., 4, 19–30, 2014.
Papazachos, B. C., Comninakis, P. E., Scordilis, E. M., Karakaisis, G. F., and Papazachos, C. B.: A catalogue of earthquakes in the Mediterranean and surrounding area for the period 1901–2010, Publ. Geophys. Laboratory, University of Thessaloniki, 2010.

SED
6, 2699–2733, 2014

Papazachos, B. C. and Papazachou C. B.: The Earthquakes of Greece, Ziti Editions, Thessaloniki, 2003 (in Greek).
Papazachos, C. B. and Nolet, G.: *P* and *S* deep velocity structure of the Hellenic area obtained by robust nonlinear inversion of travel times, J. Geophys. Res., 102, 8349–8367, 1997.
Pearce, F. D., Rondenay, S., Sachpazi, M., Charalampakis, M., and Royden, L. H.: Seismic investigation of the transition from continental to oceanic subduction along the western Hellenic Subduction Zone, J. Geophys. Res. Solid Earth, 117, 1978–2012, 2012.
Podvin, P. and Lecomte, I.: Finite difference computation of traveltimes in very contrasted velocity models: a massively parallel approach and its associated tools, Geophys. J. Int., 105, 271–284, 1991.
Sachpazi, M., Hirn, A., Clement, Ch., Laigle, M., Haslinger, F., Kissling, E., Charvis, Ph., Hello, Y., Lepine, J., Sapine, M., and Ansorge, J.: Western Hellenic subduction and Cephalonia transform: local earthquakes and plate transport and strain, Tectonophysics, 319, 301–319, 2000.
Scordilis, E. M., Karakaisis, G .F., Karakostas, B. G., Panagiotopoulos, D. G., Comninakis, P. E., and Papazachos, B. C.: Evidence for Transform Faulting in the Ionian Sea: the Cephalonia Island Earthquake Sequence of 1983, Pure Appl. Geophys., 123, 388–397, 1985.
Tarantola, A. and Valette, B.: Inverse problems = quest for information, J. Geophys., 50, 159–170, 1982.
Thurber, C. H.: Local earthquake tomography: velocities and $V_p = V_s$ – theory, in: Seismic Tomography: Theory and Practice, edited by: Iyer, H. M. and Hiahara, K., Chapman and Hall, London, 563–583, 1993.
Tiberi, C., Diament, M., Lyon-Caen, H., and King, T.: Moho topography beneath the Corinth Rift area (Greece) from inversion of gravity data, Geophys. J. Int., 145, 797–808, 2001.
Tirel, C., Gueydan, F., Tiberi, C., and Brun, J. P:. Aegean crustal thickness inferred from gravity inversion. Geodynamical implications, Earth Planet. Sci. Lett., 228, 267–280, 2004.
Tsokas, G. N. and Hansen, R. O.: Study of the crustal thickness and the subducting lithosphere in Greece from gravity data, J. Geophys. Res. Solid Earth (1978–2012), 102, 20585–20597, 1997.
Underhill, J. R.: Late Cenozoic deformation of the Hellenide foreland, western Greece, Geol. Soc. Amer. Bull., 101, 613–634, 1989.

SED
6, 2699–2733, 2014

Valkaniotis, S., Ganas, A., Papathanassiou, G., and Papanikolaou, M.:. Field observations of geological effects triggered by the January–February 2014 Cephalonia (Ionian Sea, Greece) earthquakes, Tectonophysics, doi:10.1016/j.tecto.2014.05.012, 2014.

Yem, L. M., Camera, L., Mascle, J., and Ribodetti, A.: Seismic stratigraphy and deformational styles of the offshore Cyrenaica (Libya) and bordering Mediterranean Ridge, Geophys. J. Int., 185, 65–77, 2011.

SED

6, 2699–2733, 2014

Table 1. Focal parameters of the three strong earthquakes of the January–February 2014 Cephalonia seismic sequence as preliminary calculated by NOA.

Date	Time	Lat (deg)	Lon (deg)	M_W	M_L	h (km)
26 January 14	13.55.42.7	38.2190	20.5322	6.0	5.8	16.4
26 Janaury 14	18.45.08.3	38.2282	20.4138	5.3	5.1	16.5
03 Janaury 14	03.08.44.7	38.2462	20.3958	5.9	5.7	11.3

SED
6, 2699–2733, 2014

Table 2. Distribution of horizontal (ERH) and vertical (ERZ) errors for the events relocated with several seismic velocity models.

Performance	Adopted model	Haslinger et al. (1999)	Sachpazi et al. (2000)	Hirn et al. (1996)	NOAGI
ERH < 900 m	86 %	83 %	71 %	39 %	76 %
ERH < 600 m	57 %	57 %	43 %	21 %	46 %
ERZ < 900 m	89 %	87 %	81 %	64 %	68 %
ERZ < 600 m	69 %	67 %	59 %	44 %	43 %

SED
6, 2699–2733, 2014

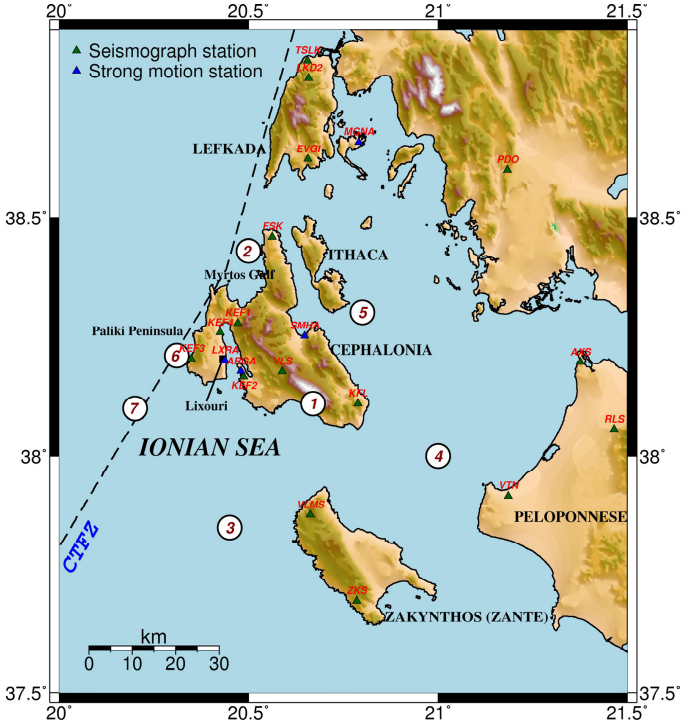

Figure 1. Location map of the study region. The Cephalonia Transform Fault Zone (CTFZ) is also indicated on the map. The seismographic stations of the Hellenic Unified Seismological Network (HUSN) are depicted with green-colored triangles and the strong motion stations with blue ones. The historical earthquakes after 1900 (Papazachos et al., 2010) are shown as white circles: (1) 24 January 1912 M6.8; (2) 9 August 1953 M6.4; (3) 11 August 1953 M6.8; (4) 12 August 1953 M6.3; (5) 12 August 1953 M7.2; (6) 17 September 1972 M6.3; (7) 17 January 1983 M7.0.

SED
6, 2699–2733, 2014

High-precision relocation of seismic sequences above a dipping Moho

V. K. Karastathis et al.

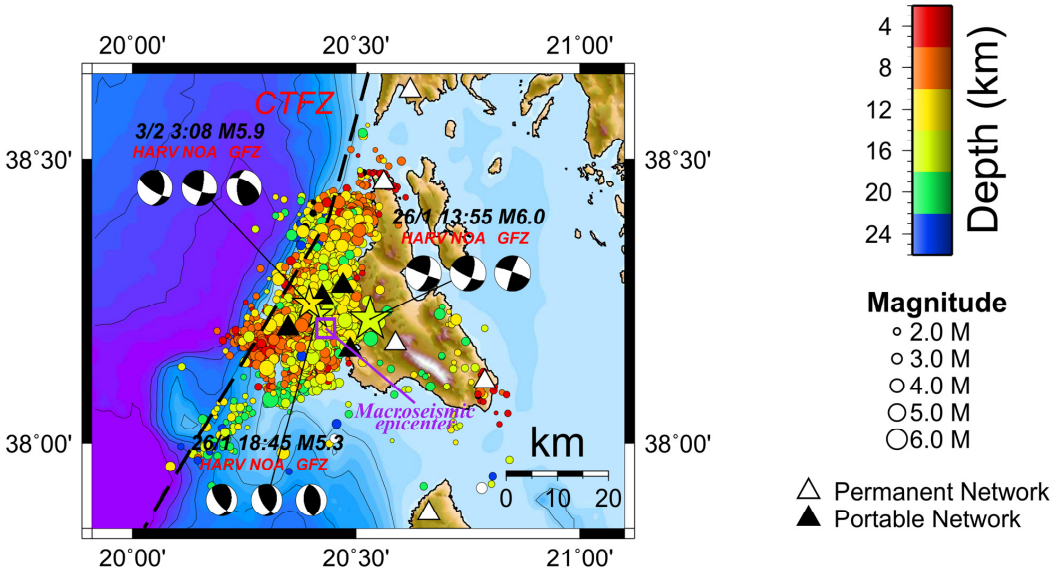

Figure 2. Map of the aftershock sequence from 26 Jnauary 2014–15 May 2014 as determined by the National Observatory of Athens. The moment tensor solutions for the largest events as calculated by Global CMT – Harvard University, USA (HARV), National Observatory of Athens (NOA) and GFZ German Research Centre for Geoscience (GeoForschungsZentrums in German) (GFZ).

SED
6, 2699–2733, 2014

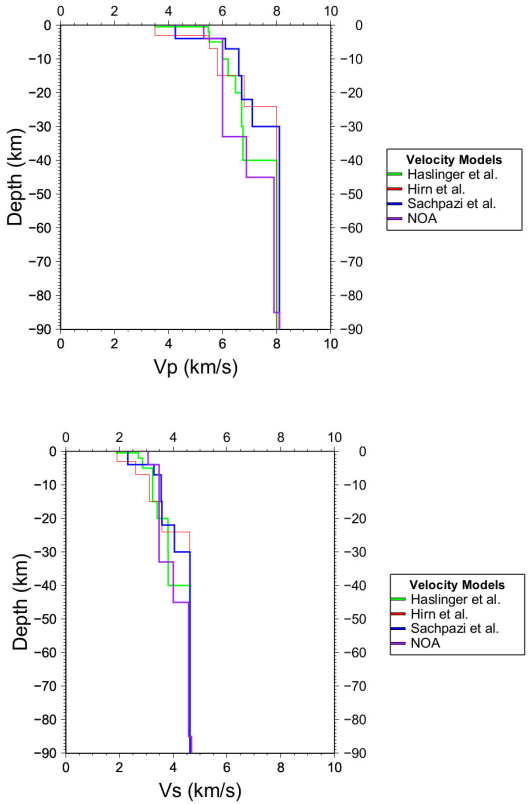

Figure 3. The seismic *P* and *S* wave velocity models tested for the relocation of the aftershock sequence. Green, blue and red correspond to velocity models proposed by Haslinger et al. (1999), Sachpazi et al. (2000), and Hirn et al. (1996), respectively. The model routinely used by NOAGI is marked in purple.

SED
6, 2699–2733, 2014

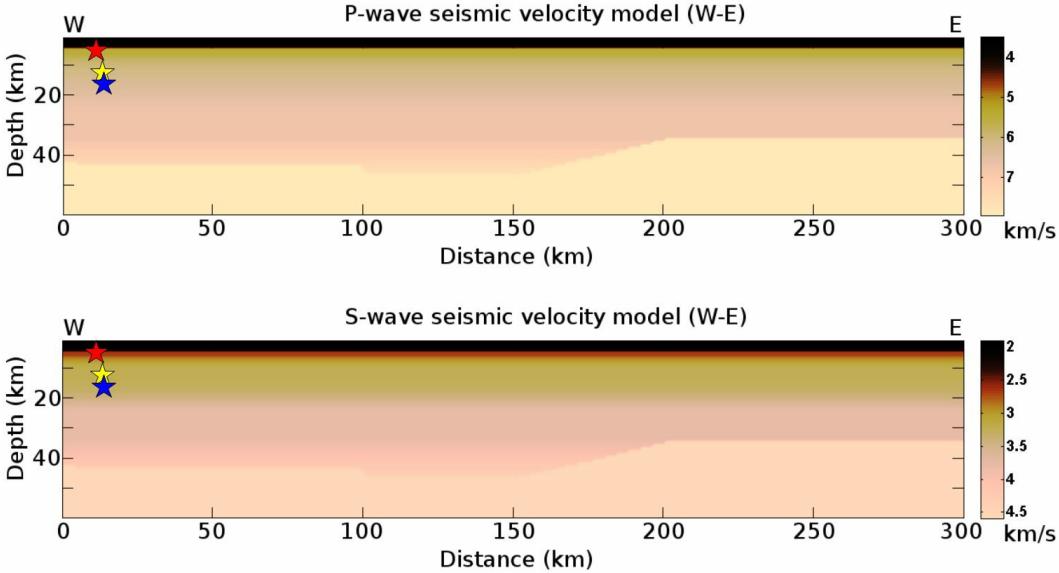

Figure 4. The 2-D velocity model tested to assess the influence of Moho structure. The Moho boundary has been based on the results of Papazachos and Nolet (1997). The position of Cephalonia is between 0–50 km. The hypocenters of the major events are shown with stars (blue for the event of 26 January 2014 (M_w6.0); yellow for the aftershock of 26 January 2014 (M_w.5.3); red for the event of 3 February 2014 (M_w5.9).

SED
6, 2699–2733, 2014

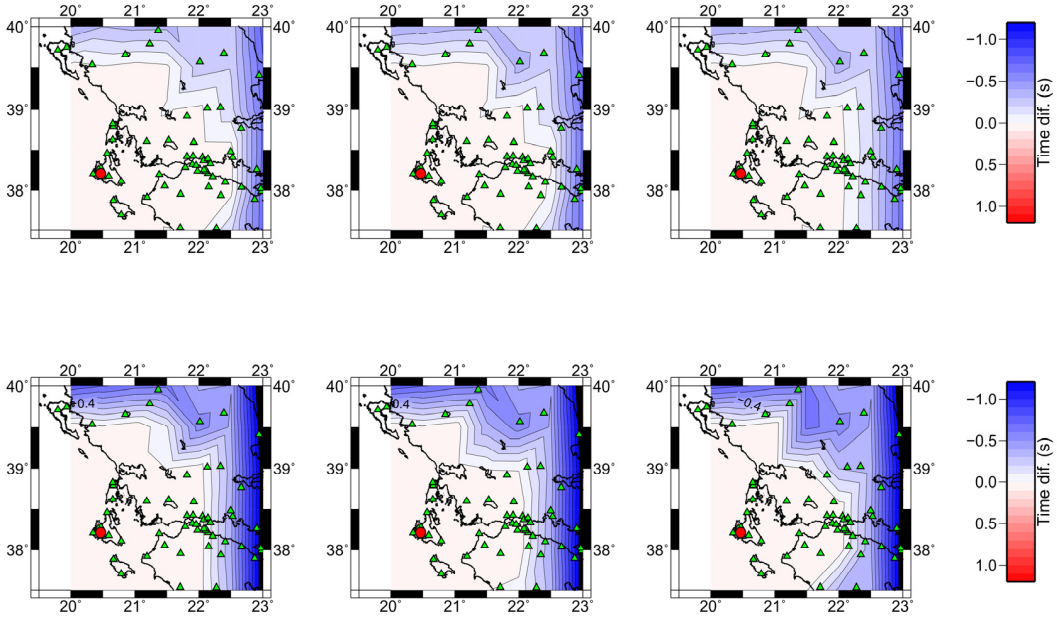

Figure 5. Time differences of *P* wave (upper panel) and S-wave (lower panel) arrivals between synthetic data calculated on the basis of the 1-D model adopted and the 2-D model based on the same 1-D model but with a non-horizontal Moho boundary. Earthquake focal depths of 5 km (left), 10 km (central) and 15 km (right) are represented. The hypothetical epicentre is shown as red circle. The errors imported in the case which does not take into account the Moho structure can be significant at long distances.

SED
6, 2699–2733, 2014

High-precision relocation of seismic sequences above a dipping Moho

V. K. Karastathis et al.

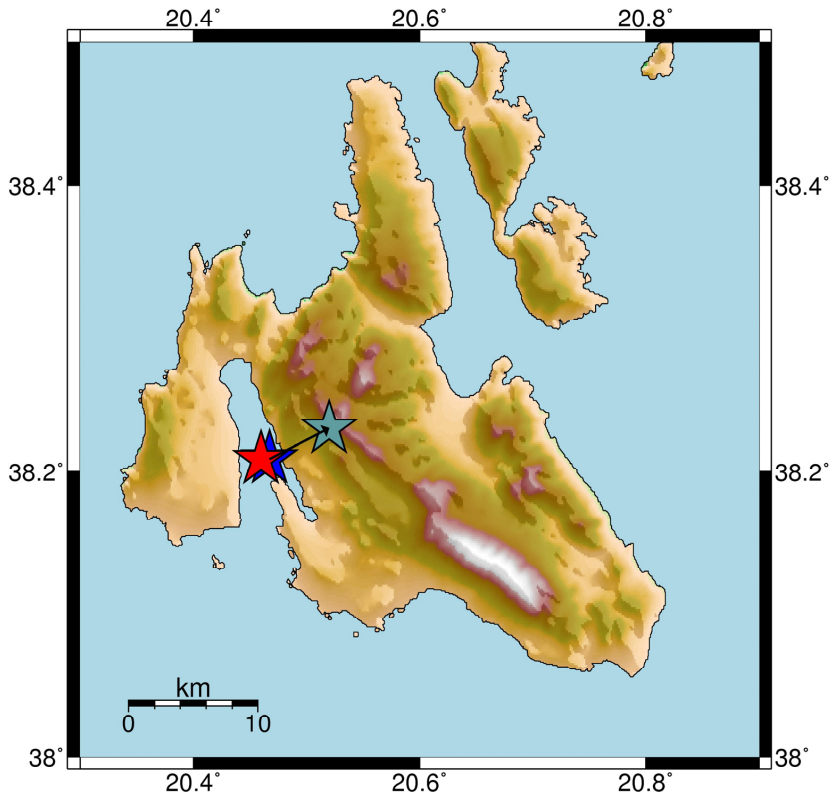

Figure 6. The epicenter of the strong earthquake (M_w6.0) of 26 January 2014 calculated with the 1-D model of Haslinger et al. (1999) (see Fig. 3) including distant phases (light blue star at the east), the same 1-D model excluding distant phases (blue star at the west), and the 2-D model (see Fig. 4) including distant phases (red star).

SED
6, 2699–2733, 2014

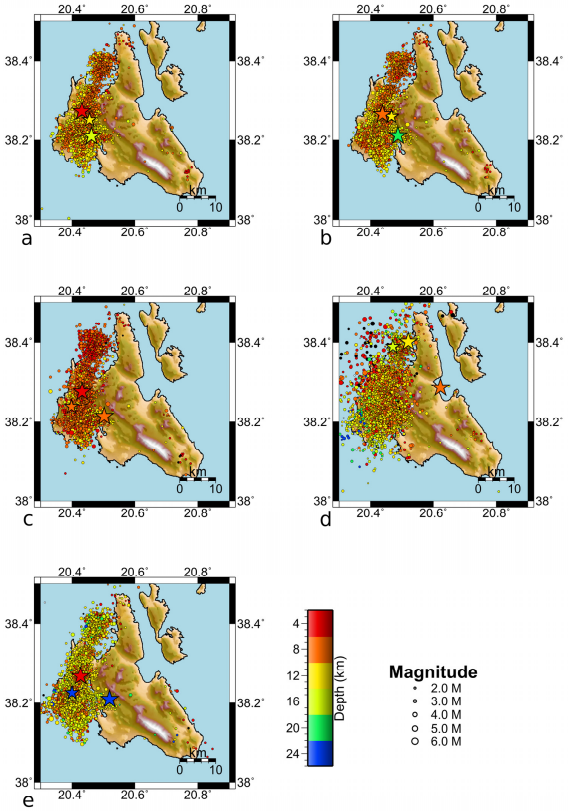

Figure 7. Relocation results by using the velocity models of **(a)** the 2-D velocity model that resembles the moho structure, **(b)** the 1-D velocity model proposed by Haslinger et al. (1999), **(c)** the 1-D velocity model proposed by Sachpazi et al. (2000), **(d)** the 1-D velocity model proposed by Hirn et al. (1996), **(e)** the 1-D velocity model used by NOAGI for the daily seismic monitoring.

SED
6, 2699–2733, 2014

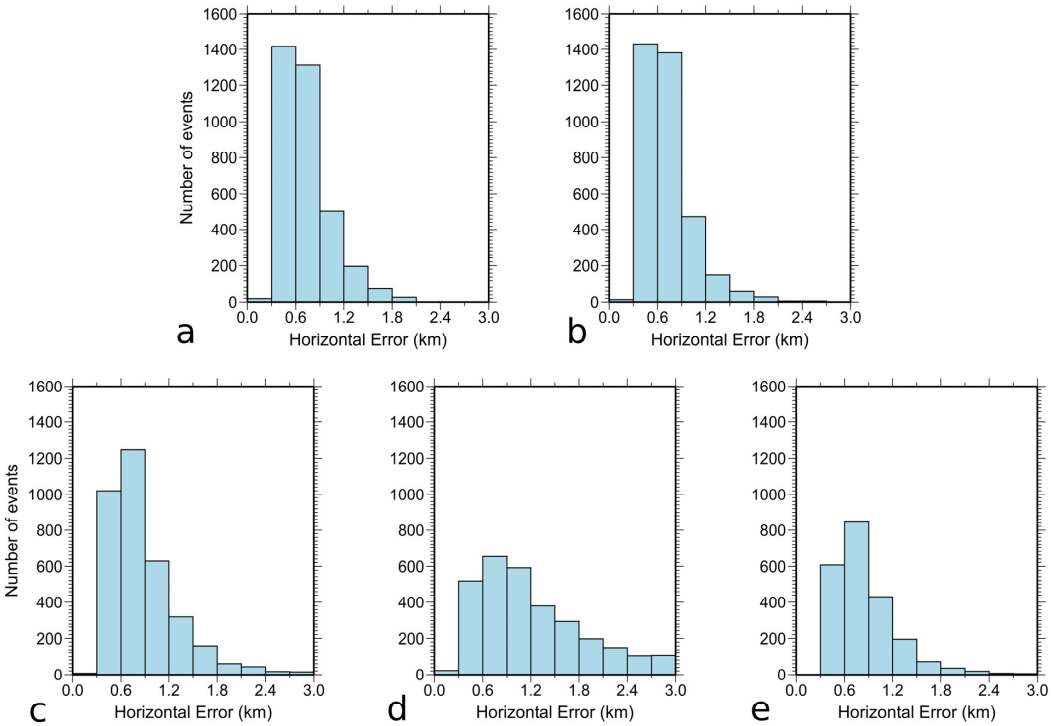

Figure 8. Distribution of the epicenter horizontal error of the relocated Cephalonia 2014 earthquake sequence up to15.5.2014 for different seismic velocity models: **(a)** adopted 2-D model which is a modification – of the Haslinger et al. (1999) model; **(b)** Haslinger et al. (1999); **(c)** Sachpazi et al. (2000); **(d)** Hirn et al. (1996); **(e)** model routinely used in the daily seismic monitoring by NOAGI.

SED
6, 2699–2733, 2014

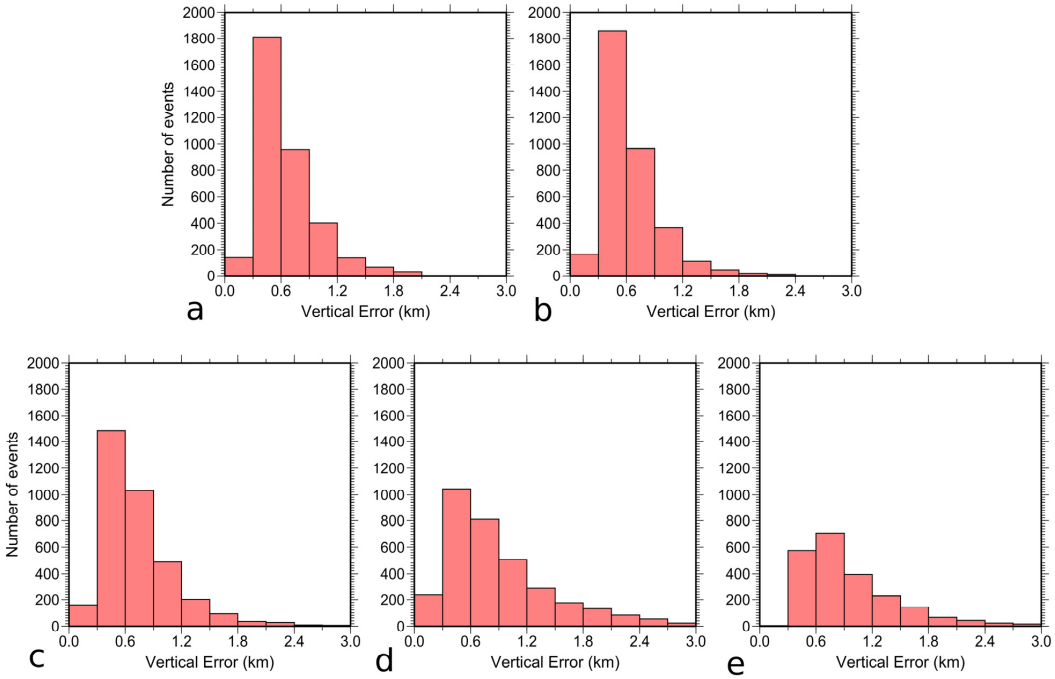

Figure 9. As Fig. 8 for the vertical epicenter error.

SED
6, 2699–2733, 2014

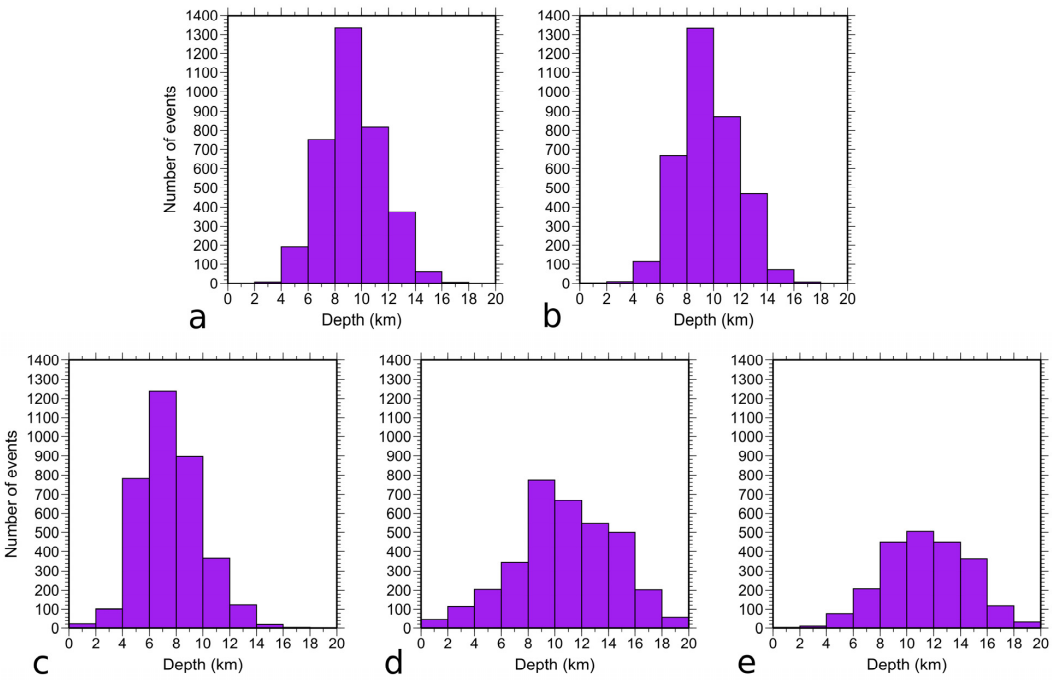

Figure 10. Distribution of hypocentral depth of the relocated Cephalonia 2014 earthquake sequence up to 15 May 2014 for different seismic velocity models: **(a)** adopted 2-D model which is a modification – of the Haslinger et al. (1999) model; **(b)** Haslinger et al. (1999); **(c)** Sachpazi et al. (2000); **(d)** Hirn et al. (1996); **(e)** Model routinely used in the daily seismic monitoring by NOAGI.

SED
6, 2699–2733, 2014

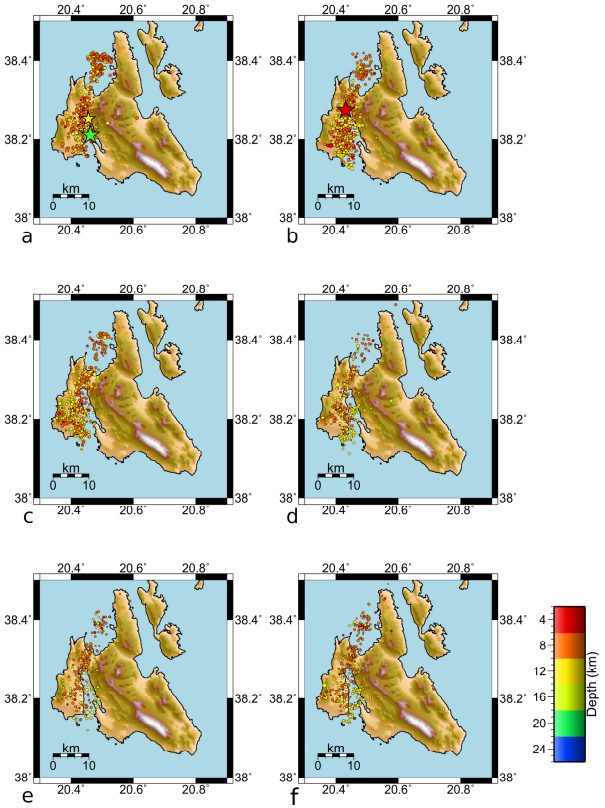

Figure 11. Space-time evolution of the Cephalonia 2014 sequence. The maps show the aftershocks with one week time interval (from **a** to **f**) beginning from 26 January 2014 to 26 March 2014.

SED
6, 2699–2733, 2014

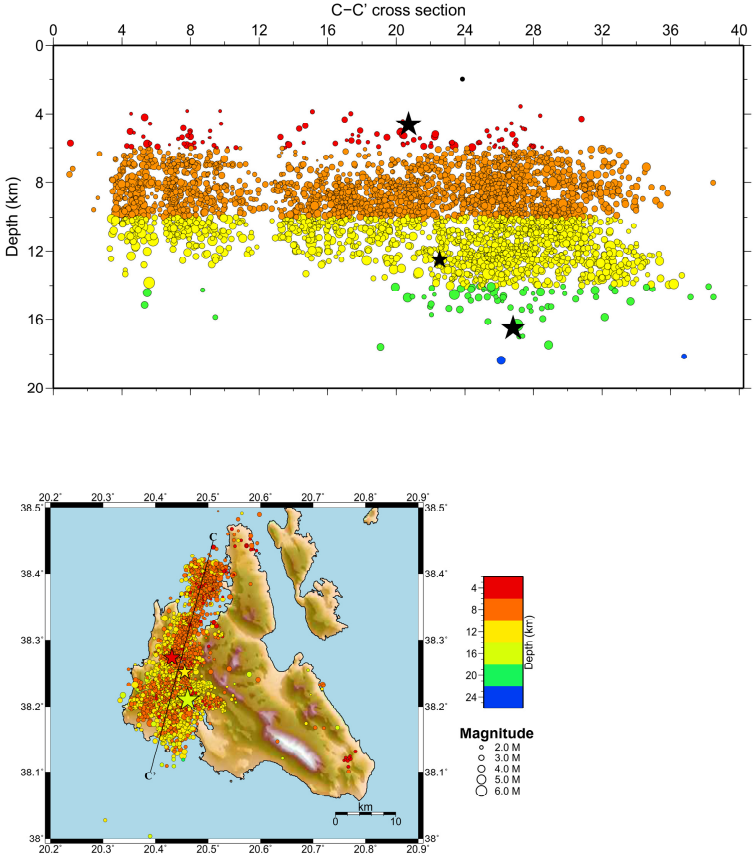

Figure 12. Vertical section of the aftershock sequence during 26 January 2014 to 15 May 2014 and its location map.

SED
6, 2699–2733, 2014

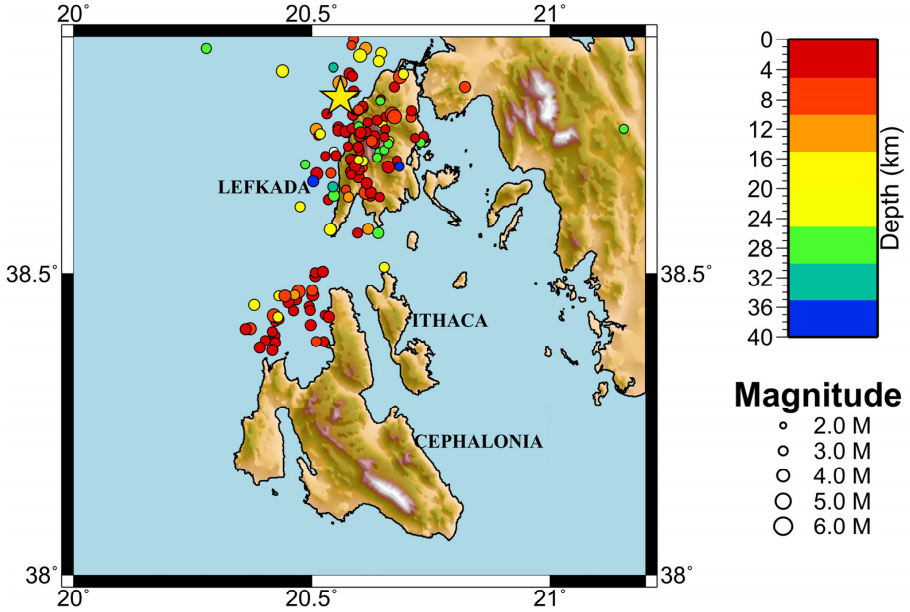

Figure 13. Map showing the Lefkada 2003 aftershock sequence as located by NOAGI. Only the events located with at least 6 phases are shown.

SED
6, 2699–2733, 2014

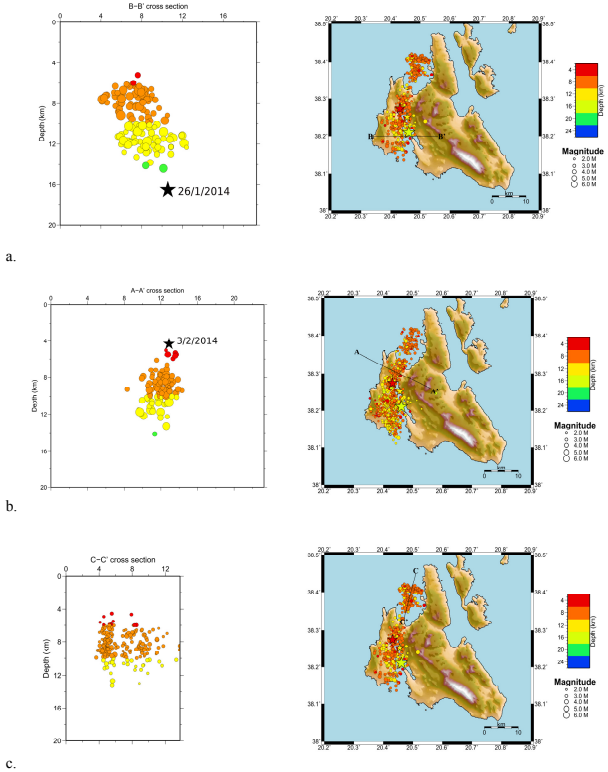

Figure 14. Vertical sections of the aftershock sequence and their location maps **(a)** The section depicts the hypocenters (with GAP < 180°) between 26–30 January 2014b) The section depicts the hypocenters (with GAP < 180°) between 3–8 February 2014c) The section depicts the hypocenters (with GAP < 180°) between 26–30 January 2014.

SED
6, 2699–2733, 2014

High-precision relocation of seismic sequences above a dipping Moho

V. K. Karastathis et al.